The investigation of the luminescent structure of thallium-doped cesium iodide (CsI:Tl) basing on the first-principles coupled with spectral analysis

IOP Publishing Journal of Physics: Condensed Matter
J. Phys.: Condens. Matter **34** (2022) 215901 (8pp) https://doi.org/10.1088/1361-648X/ac5a91

The investigation of the luminescent structure of thallium-doped cesium iodide (CsI:Tl) basing on the first-principles coupled with spectral analysis

T J Gao[1], H D Wang[1], Jing-Bin Lu[1,*], Song Yue[2], Sun Chao[1] and De-fang Duan[1,3]

[1] College of Physics, Jilin University, Changchun 130012, People's Republic of China
[2] Changchun Institute of Optics, Fine Mechanics and Physics, Chinese Academy of Sciences, Changchun 130033, People's Republic of China
[3] State Key Laboratory of Superhard Materials, Jilin University, Changchun 130000, People's Republic of China

E-mail: ljb@jlu.edu.cn

Received 19 November 2021, revised 11 February 2022
Accepted for publication 3 March 2022
Published 23 March 2022

Abstract

The luminescent structure of thallium-doped cesium iodide (CsI:Tl) and the behavior of electrons during luminescence are studied at great length based on the conventional first-principles calculation combined with ordinary spectroscopic analysis befittingly in this work. The hybrid functionals based on a screened Coulomb potential (HSE) is used to visualize the energy band structure of the experimental sample's system, and the corresponding relationship between the transition behavior of CsI:Tl energy levels and the spectrum is studied more accurately. We show the complete energy conversion process clearly, which involves the crystal beginning to receive the energy of a photon until the moment of de-excitation. All the fluorescence process is completed by Tl^+ ions that replace Cs^+ ions. Our results verify and complement the previous theories and potentially provide important references for the adjustment and design of the detectors and imaging equipment in different fields.

Keywords: the first-principles calculation, CsI(Tl), spectra

(Some figures may appear in colour only in the online journal)

1. Introduction

Scintillation detectors are widely used in high-energy physics, nuclear medicine, geophysical exploration, and other fields. Inorganic scintillators are usually coupled with photomultipliers as scintillation detectors [1, 2]. As the core component of these instruments, scintillators have a very important research position, which is responsible for converting incident photons into fluorescent photons. Alkali halide scintillators (mainly NaI and CsI families) play a particular role due to their comparatively high efficiency and low cost of production [3].

The luminescence mechanism of CsI(Tl) is relatively mature, some works have proposed some forms of the light-emitting structure of CsI:Tl, but the way to verify the conclusion is different [4–6]. Therefore, we chose CsI(Tl) as the sample for the study, hoping to verify the feasibility of our research method. It is important to have a clear understanding of the mechanism of scintillator emission. On the basis of previous research, a new research approach was adopted to analyze its luminescence mechanism in this work. However, it

* Author to whom any correspondence should be addressed.

is difficult to study the mechanism of scintillator under radiation irradiation in the field of nuclear physics, so our work starts from the near-ultraviolet light source. CsI(Tl) belongs to a simple cubic crystal system with a simple periodic structure, which is suitable for first-principles calculation.

A series of intermediate processes exist in the process of crystal receiving energy and producing light. Although enough spectral data have been measured by predecessors and a lot of in-depth studies have been done on the mechanism of its luminescence, the experimental values and theoretical values have not been matched. In 1995, reference [5] provided a brief energy level diagram and some parameters to explain the spectrum measured in their experiment, but did not actually calculate the band structure of CsI:Tl. Schematic diagram of the optically stimulated charge-transfer processes in CsI:Tl was presented and demonstrated in reference [7] during 2002, the energy relaxation model in alkali metal halides doped with thallium-like activators was speculated in reference [3] later. However, these conclusions are only obtained from experimental data and are not supported by energy level data. In this paper, a new way to study the luminescence mechanism of scintillators is provided, and it is expected to verify or supplement the conclusions obtained from the research and analysis. The first-principles calculation results are combined with experimental data in this work to verify and supplement the previous theories in order to better understand the luminescence mechanism of CsI:Tl. The existence form of Tl element responsible for luminescence in the system was confirmed, and the excitation and de-excitation modes of extranuclear electrons were analyzed and discussed. Our work combines traditional spectroscopy methods with density functional theory, which can be used to study the microscopic luminescent structure of scintillators, to gain a further understanding of the luminescence mechanism of various crystals. Then, more accurate performance parameters of scintillators such as light yield and decay time are obtained. According to the understanding of the luminescence mechanism of scintillators, the corresponding relationship between rays and channels can be modified to obtain more real ray information, such as energy and intensity, etc.

2. Experimental procedures

The characteristics of pure cesium iodide and cesium iodide doped with thallium have already been investigated earlier. In this paper, experimental data and theoretical calculation results for CsI and CsI(TI) are presented. All the experimental samples in this work are several bulk single crystals purchased from Shanghai Ucome New Material Co., Ltd. The presence of thallium in the samples was confirmed by ICP-MS, and the form of Tl in CsI(Tl) was predicted by XRD. Excitation and emission spectra were measured to determine the excitation wavelength and emission wavelength of the sample. Finally, the fluorescence attenuation time of the sample was determined by measuring the fluorescence lifetime.

The RIGAKU SmartLab SE placed in the Physics College of Jilin University was used to perform an x-ray diffraction (XRD) test on CsI(Tl) and CsI powder, using Cu target radiation, $\lambda(\kappa\alpha_1) = 0.154\,0598$ nm, $\lambda(\kappa\alpha_2) = 0.154\,4426$ nm. The tube voltage was 40 kV, the tube current was 30 mA, the scanning mode was continuous scanning, the scanning speed was 1°/min, and the scanning range was 10–60°. All the above tests were carried out at room temperature. The types of elements present in the sample were determined by inductively coupled plasma mass spectrometry (iCAP Qc).

The excitation spectra and the photoluminescence spectra were measured on an F-7000 Fluorescence Spectrophotometer. The luminescence decay time spectrum was measured on the FL920 fluorescence decay spectrometer. All the spectral data were measured in Changchun Institute of Optics, Fine Mechanics and Physics, Chinese Academy of Sciences.

3. First-principles calculation

Theoretical calculations were performed on CsI and CsI(Tl) using the first-principles calculation method based on the hybrid density functions to study the band structure and the density of states of CsI and Cs(Tl). The density of states and the band structure of pure CsI is calculated in order to verify the accurate degree of this method and compare the changes after doping Tl. The method includes a certain amount of Hartree–Fock (HF) exchange, and has further improved upon the PBE results [8, 9]. The hybrid functionals based on a screened Coulomb potential (HSE) algorithm is used in the theoretical calculation, which avoids the problem of underestimating the band gap compared with Perdew–Burke–Ernzerhof (PBE).

All the calculations have been done using CASTEP (Cambridge Serial Total Energy Package) [10]. We expanded the valence electronic wave functions in a plane-wave basis set up to an energy cutoff of 440 eV for CsI and an energy cutoff of 10 eV for CsI:Tl. The electron–ion interaction is described by the norm conserving pseudo-potentials. The convergence accuracy is set to ultra-fine. The convergence accuracy in the iteration process is 5×10^{-7} eV/atom and the K points are set to $2 \times 2 \times 2$ and $1 \times 1 \times 1$ for CsI and CsI:Tl separately. When calculating the density of states, the Brillouin region is sampled by Monkhorst–Pack method, and the convergence accuracy is 5×10^{-7} eV/atom. The calculation models are shown in figure 3.

4. Results and discussion

4.1. Lattice parameters by XRD and ICP-MS analysis

A small amount of powder sample was ground from massive crystals and dissolved in distilled water to make liquid samples, using ICP-MS to detect the types of cations contained in the samples. The average concentrations of Na, Tl, and Cs are 1.303 ppb, 36.158 ppb, and 115858.586 ppb respectively. This indicates that Tl element is present in the crystal, although there is a trace of Na element, the content of Na compared with other elements is extremely weak.

After confirming the existence of Tl, the form of Tl in the lattice was determined by XRD. The background was suppressed by prolonging the measurement time, we detected

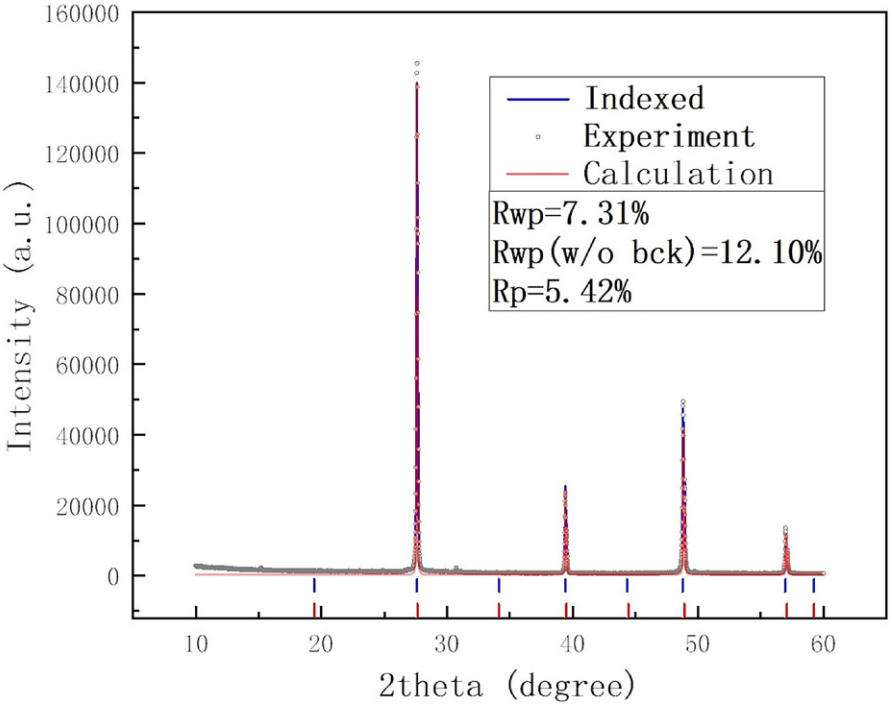

Figure 1. XRD pattern of the ground powder from large CsI(Tl) single crystals.

the weak small peak caused by the presence of Tl elements. Figure 1 is a local magnification of the XRD curve. The diffraction peaks caused by Tl element in XRD curves can be observed, which indicates that Tl combines with other elements to form crystalline phase. Due to the low content of Tl, the intensity of XRD diffraction peak formed is very weak. Although the peak intensity measured in a short time is extremely weak, it can be seen that the peak intensity increases significantly with the extension of the measurement time. It means that they are not the background but the diffraction peaks.

The XRD measurements were used for derivation of the lattice constants, and the deviation between theoretical simulation and experimental results was minimized. Then obtain the lattice structure closer to the actual sample based on the processed experimental data. The XRD pattern of CsI(Tl) powder, which has been refined, is shown in figure 2. We reproduce the XRD pattern of the sample theoretically and compared with the experimental data to prove the reliability of the calculation model [11]. It can be verified from the data that there is a good agreement between the theoretical curve and the experimental graph, diffraction peaks due to Tl elements are also simulated. Thus, it is speculated that the Tl exists in the form of substitution doping. And the crystal cell parameters obtained from the processed data are $a = 4.555\,162\,00$, $b = 4.555\,162\,00$, $c = 4.569\,099\,00$, $\alpha = \beta = \gamma = 90°$.

We construct theoretical simulation models of CsI and CsI(Tl). The computational model of CsI(Tl) was constructed based on the unit cell parameters obtained by the analysis results of XRD refinement and ICP-MS. The supercell structure of CsI(Tl) is shown in figure 3(b).

4.2. PLE spectra and PL spectra

Excitation and emission spectra of bulk crystal samples were measured in this work. Even for the same type of crystal, the peaks of the excitation spectrum and the emission spectrum will have a certain deviation due to the influence of the doping process of the sample and other factors. In order to cooperate with the previous computational model derived from experimental data, we measured the excitation and emission spectra of the same sample. Excitation spectrum shows the photoluminescence wavelength of the sample, and emission spectrum shows the photoluminescence wavelength under the excitation of each peak value in the excitation spectrum.

The conclusion that can be drawn from the excitation spectra data (figure 4(a)) is that the trends of the excitation spectra which were measured at three wavelengths were roughly the same, but the intensity is different. While the intensity of the $\lambda_{em} = 410.6$ nm is the lowest, and the $\lambda_{em} = 514.2$ nm is the highest. The spectral composition of the luminescence induced by UV-light in CsI(Tl) at room temperature is shown in figure 4(b). We found two bands peaking at 410.50 nm and 514.20 nm, among which the peak at 514.2 nm the central wavelength of the scintillator sample. Fast intrinsic luminescence peaking at 300 nm has previously been observed in CsI, and the central wavelength is redshifted by thallium doping [3, 12, 13]. The position of the central wavelength is quite different from previous results. The result of ICP-MS shows that the proportion of Tl is 0.02%, and the content of the Na element was only 0.006%. We speculate that trace amounts of sodium are responsible for this phenomenon.

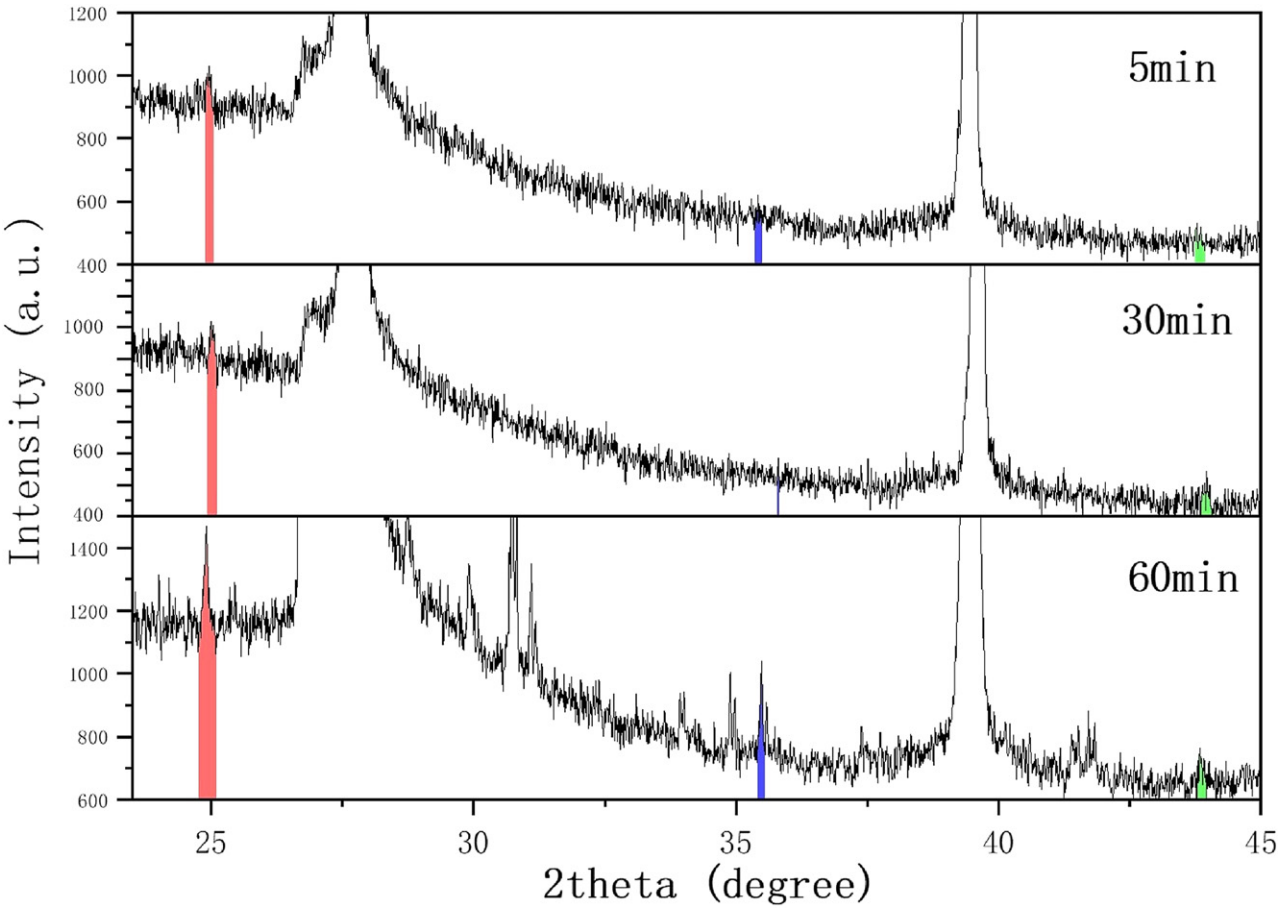

Figure 2. Magnified partial XRD curves of the CsI(Tl) sample, respectively at 5 min, 30 min, 1 h time measurement.

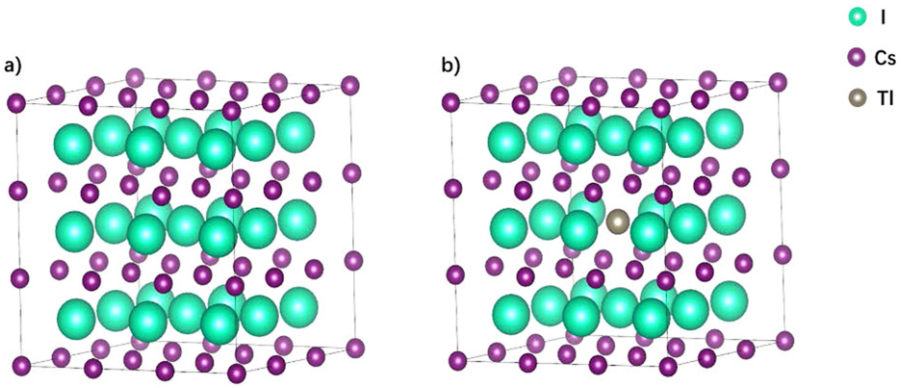

Figure 3. Crystal structures of (a) CsI, and (b) CsI(Tl). The green, violet, and brown balls represent iodine, cesium, and thallium atoms, respectively.

4.3. Band and density of states

From the calculated band structure of CsI(Tl), the contribution of elements to band composition and energy level distribution can be obtained. The calculation of the density of states helps to obtain the element's contribution to the band. By analyzing these data, the band structure corresponds with the spectral data. The luminescence mechanism of CsI(Tl) can be analyzed by studying the corresponding relationship between band structures and spectra. Figures 5 and 6 severally show the calculated band structures of CsI and CsI(Tl). Both of them are calculated by using HSE method. Compared with the PBE method, the HSE method applies the screened Coulomb potential to screen the long-range part of HF exchange [8]. As a result, it drastically reduces the cost of calculations for large periodic systems and also weakens the problem of PBE underestimating the band gap.

The band gap of pure CsI is 5.216 eV in this paper, while the experimentally measured band gap in literature [14] is about 5.18 eV. It indicates that this method has good accuracy to

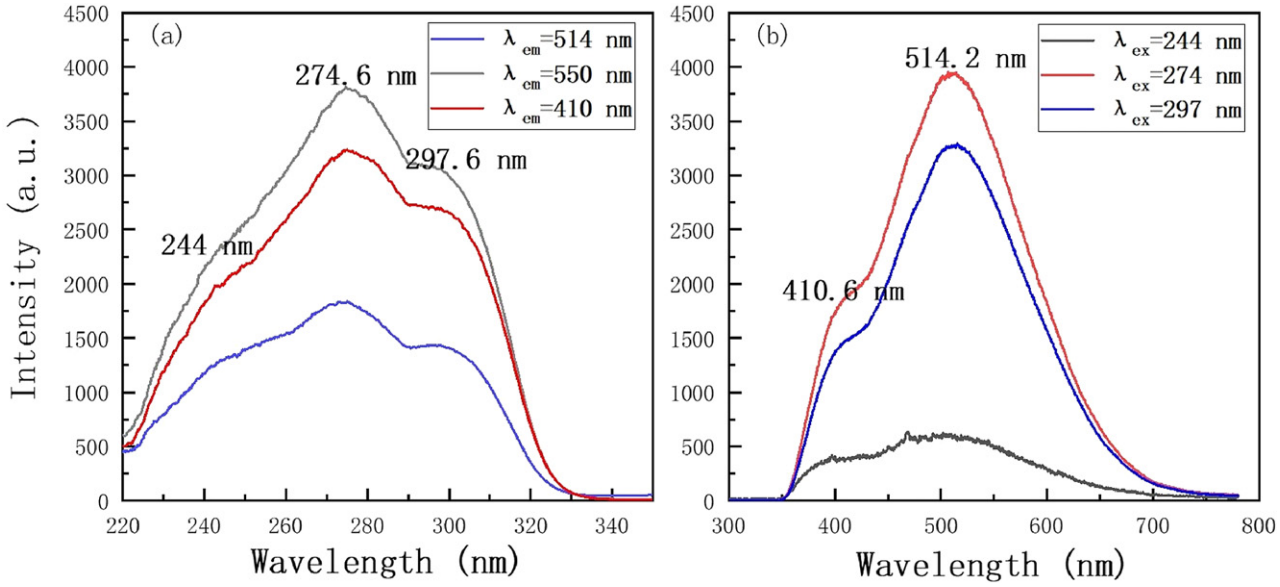

Figure 4. (a) Excitation spectra of the CsI(Tl) sample monitored at 410 nm, 514 nm, and 550 nm. (b) UV and visible emission spectra of CsI(Tl) under 244 nm, 274 nm, and 297 nm excitation.

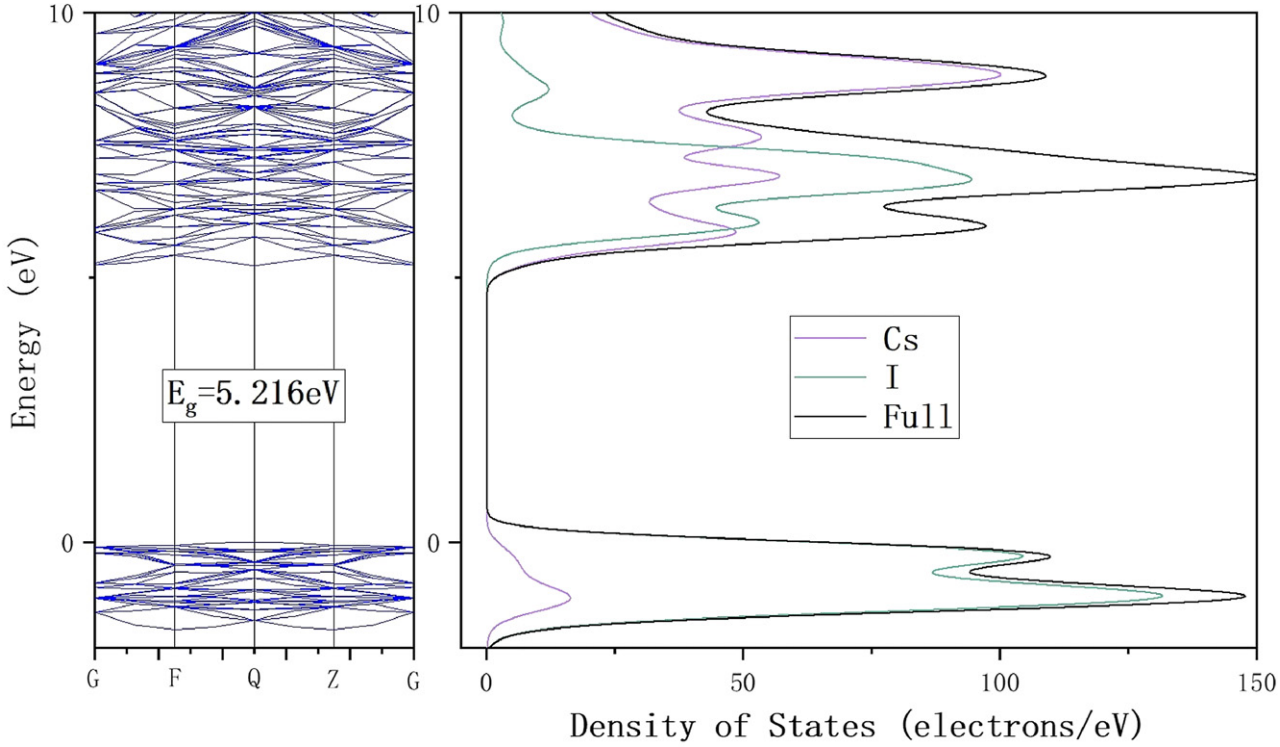

Figure 5. HSE calculated band structures and corresponding density of states for CsI (E_g = 5.216 eV). The states colored in violet and green are for cation Cs^+, and I^-, respectively.

calculate the CsI(Tl) within the allowable range of error. And it can be seen that the bandgap of CsI(Tl) is more narrow than CsI. Both CsI and CsI(Tl) exhibit indirect bandgap, but the difference is that if Cs^+ cations are replaced by Tl^+ ions, the conduction band is made up of both Tl-6p, I-5s, and Cs-5p orbitals while the valence band has a predominantly I-5p character with some mixing of Cs-5p and Tl-6s orbitals. And the CBM no longer derives from the Cs^+ 6s orbital, the conduction band minimum (CBM) is mainly derived from Tl 6p orbitals. Thus, concludes from the density of states that Tl^+ contributes to the bottom of the band rather than Tl^+ causing the formation of gap energy levels. And it can be inferred that thallium doping in CsI reduces the band gap of CsI crystal from 5.216 eV to 4.308 eV, mainly due to the reduction of impurity conduction band caused by activator Tl^+. The parity of the bottom of the conduction band will change accordingly. The valence

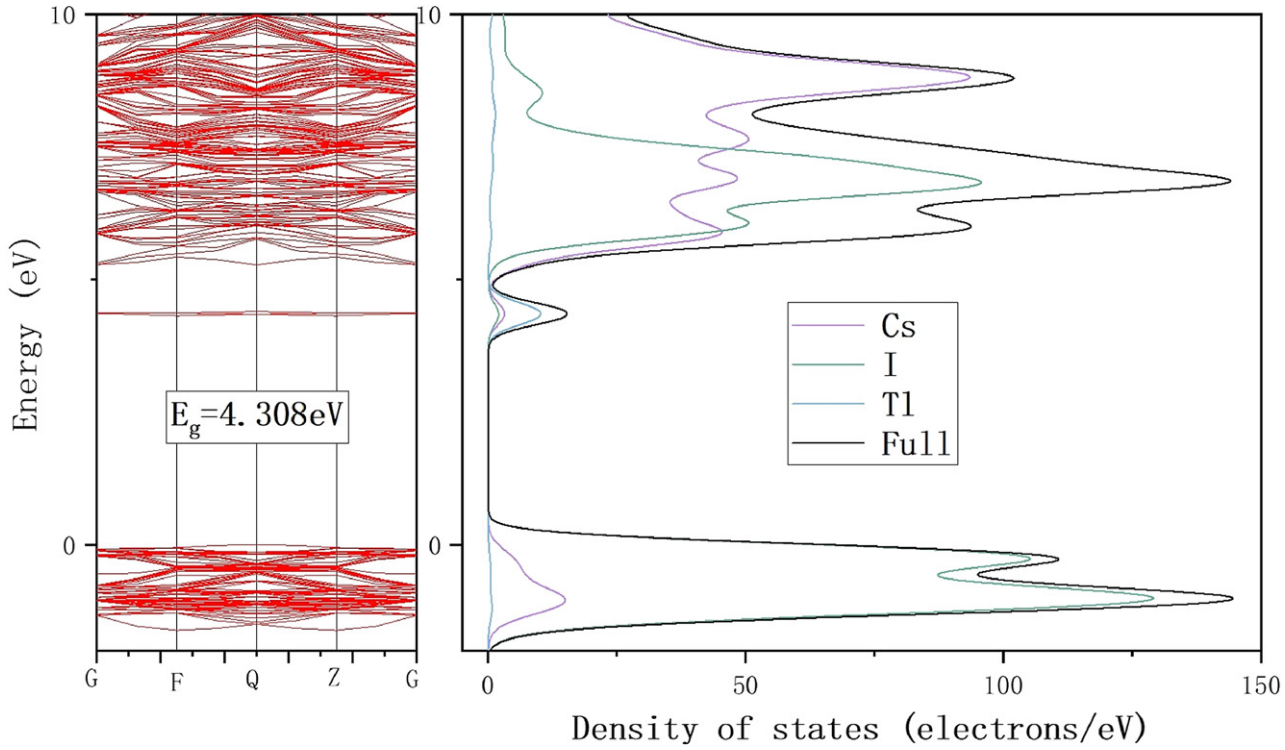

Figure 6. HSE calculated band structures and corresponding density of states for CsI(Tl) ($E_g = 4.308$ eV). The states colored in violet, blue, and green are for cation Cs^+, cation Tl^+, and I^-, respectively.

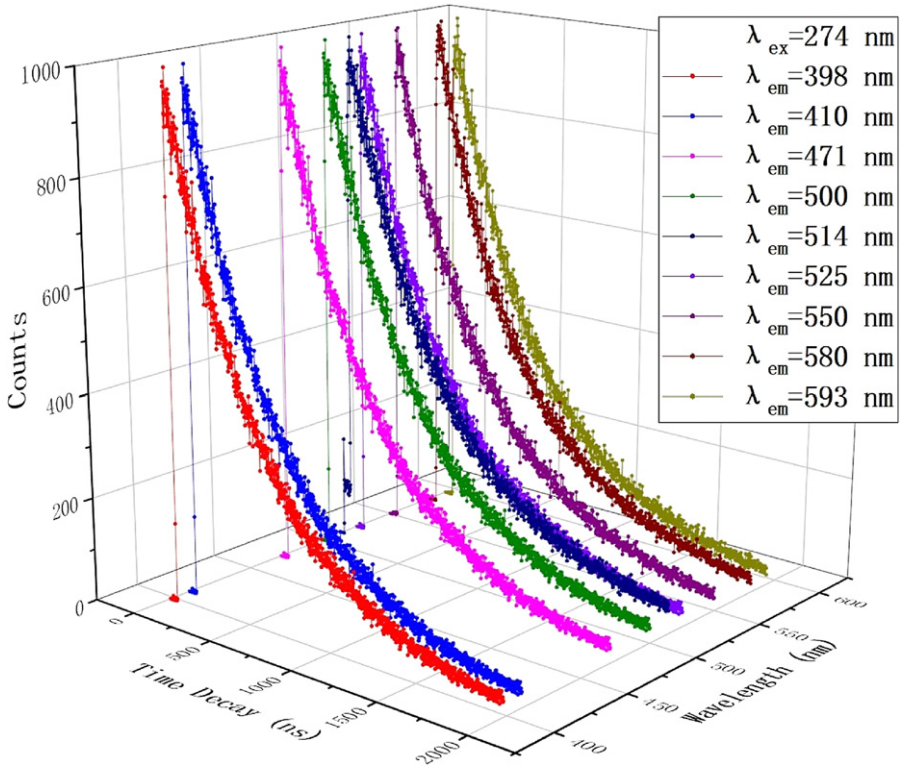

Figure 7. Time decay curves of the CsI(Tl) sample were monitored at different emission wavelengths under 274 nm excitation.

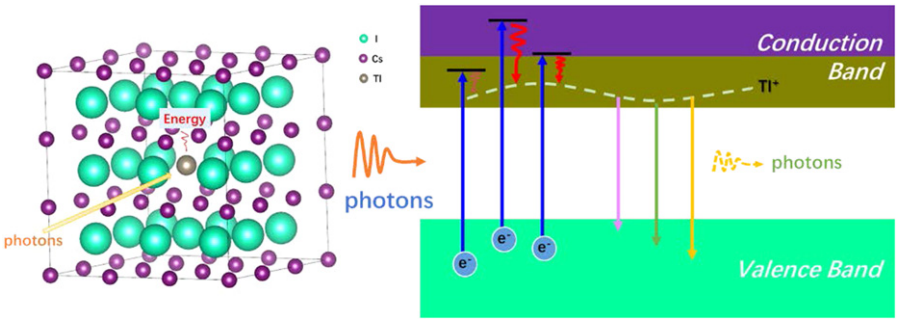

Figure 8. Diagram of luminescence kinetics process.

band maximum (VBM) consists of I 5p orbitals and lies at Q point [6, 15–19].

4.4. Time decay

The time-resolved decay curves of the luminescence registered at several emission wavelengths at room temperature are shown in figure 7. The number of components responsible for luminescence can be determined by measuring the fluorescence lifetime of the sample at different emission wavelengths. All the oscillograms of luminescence pulses in visible spectral regions were monitored at the excitation wavelength of 274 nm. It can be seen that the kinetic is characterized by the presence of monotonic decay. The obtained luminescence lifetime is 574.65 ns for all emission wavelengths which are chosen by us. And the obtained decay curves were fitted with a one-component exponential decay function. The above indicates that there is at most one exponential component in the scintillation decay, which means that all the emissions come from the same excited state [8]. Radiative time of excited Tl activator centers was close to experimentally obtained values for CsI(Tl) under intra center photoexcitation, which was equal to 10^{-6} s [3].

5. Analysis and interpretation of results

XRD and ICP-MS were used to determine the existing forms of Tl elements and the lattice structure of the actual sample was constructed in this work. Then the energy band structure of the CsI(Tl) sample was calculated using the HSE method. By analyzing the correspondence between spectra and band structure, it is concluded that CsI(Tl) has only one type of luminescent center. Besides the Tl doping model proposed in this paper, no other luminescent structure exists in CsI(Tl). We get some conclusions by analyzing the theoretical calculation results and spectral data. The band structure of CsI(Tl) has changed compared with that of pure CsI. The composition of the conduction band and the origin of the orbitals at the bottom of the conduction band are different, which have been described in the results and discussion. The bandgap type of CsI(Tl) is an indirect bandgap. It means that the conservation of momentum and energy needs the assistance of phonons. Due to the influence of Tl, the bands contributed by Cs move upward, and the parity at the bottom of the guide band also changes. The three peaks of the excitation spectrum are used as the excitation wavelength to stimulate the scintillator respectively, aiming to explore the excitation path and luminescent deexcitation path of CsI(Tl) crystals. The shapes of the emission spectra obtained are almost the same, which only show a strong central peak position and an accompanying weak shoulder peak, indicating that CsI(Tl) crystal has only one luminous path as long as it is excited by a light source in the excitation wavelength range that can make CsI(Tl) crystal excited to produce visible light. The corresponding relationships between the peak positions and energy states in the excitation spectrum can be obtained by analyzing the energy band diagram. The excitation peak peaking at 244 nm corresponds to the transition between Cs-p and I-p. The strongest excitation peak peaking at 274.6 nm and the second strongest peak peaking at 297.6 nm both correspond to the transition between Tl-d and I-p.

The inference from the above results is as follows and our hypothetical process is shown in figure 8. The existence mode of Tl elements was determined to be substitution doping by analyzing the XRD curve and ICP-MS. The shapes of the obtained excitation spectrum curves under different emission wavelengths are the same, and the shapes of the obtained emission spectrum curves under different excitation wavelengths are also the same. At the same time, except for the decay time curves at the emission peaks, the shapes of the measured decay curves under a series of randomly selected bands are nearly the same and there is only one component. It demonstrates the point made in this paper. After the crystal receives photons with different energies, the corresponding electrons in the valence band will relax to the same energy band contributed by Tl^+ after being excited. Then the fluorescence process is completed by de-excitation from this energy band. The valence electrons originally in the ground state of CsI(Tl) crystal transition to the energy levels corresponding to the absorbed energy values after receiving energy. Through lattice relaxation, they reach the conduction band contributed by Tl^+ ions. All valence electrons that transition to the energy levels of these Tl^+ ions deexcite back to the ground state through the same process releasing visible light photons.

In conclusion, CsI(Tl) only passes through one optical path during the entire fluorescence process. The electrons in the valence band are excited and transition to higher energy states and relax to the energy bands mainly contributed by Tl^+ ions which are doped only by substitution. The emission process is mainly completed by this part of the electrons.

Funding

National Natural Science Foundation of China (U1867210).

Disclosures

The authors declare no conflicts of interest.

Data availability statement

All data that support the findings of this study are included within the article (and any supplementary files).

ORCID iDs

T J Gao https://orcid.org/0000-0002-7279-7691
H D Wang https://orcid.org/0000-0001-5446-7982
Jing-Bin Lu https://orcid.org/0000-0002-7518-7637
De-fang Duan https://orcid.org/0000-0002-6878-1830

References

[1] Yao Z *et al* 2020 *Opt. Mater.* **105** 109964
[2] Weber M J 2004 *Nucl. Instrum. Methods Phys. Res.* A **527** 9–14
[3] Gridin S, Belsky A, Dujardin C, Gektin A, Shiran N and Vasil'ev A 2015 *J. Phys. Chem.* C **119** 20578–90
[4] Yakovlev V and Trefilova L 2020 *J. Lumin.* **223** 117183
[5] Nagirnyi V, Stolovich A, Zazubovich S, Zepelin V, Mihokova E, Nikl E, Pazzi G P and Salvini L 1995 *J. Phys.: Condens. Matter.* **7** 3637–53
[6] Yakovlev V, Trefilova L, Meleshko A, Alekseev V and Kosinov N 2014 *J. Lumin.* **155** 79–83
[7] Dexter D L 1956 *Phys. Rev.* **101** 48–55
[8] Heyd J *et al* 2003 *J. Chem. Phys.* **18** 118
[9] Perdew J P *et al* 1996 *Phys. Rev. Lett.* **77** 18
[10] Payne M C *et al* 1992 *Rev. Mod. Phys.* **64** 4
[11] Hoon K Y *et al* 2021 *Nat. Photon.* **15** 148–55
[12] Nishimura H, Sakata M, Tsujimoto T and Nakayama M 1995 *Phys. Rev.* B **51** 2167–72
[13] Belsky A N, Vasil'ev A N, Mikhailin V V, Gektin A V, Martin P, Pedrini C and Bouttet D 1994 *Phys. Rev.* B **49** 13197–200
[14] Guo-Hao R *et al* 2017 *J. Inorg. Mater.* **32** 2
[15] Weiwei M *et al* 2017 *J. Phys. Chem. Lett.* **8** 2999–3007
[16] van Loef E *et al* 2021 *Nucl. Instrum. Methods Phys. Res.* A **995** 165047
[17] Babin V, Kalder K, Krasnikov A and Zazubovich S 2002 *J. Lumin.* **96** 75–85
[18] Mollenauer L F *et al* 1983 *Phys. Rev.* B **27** 5332
[19] Ranfagni A *et al* 1983 *Adv. Phys.* **32** 823–905